PEDS Advance Access published April 9, 2010

Protein Engineering, Design & Selection pp. 1–8, 2010
doi:10.1093/protein/gzq023

A non-natural variant of human lysozyme (I59T) mimics the *in vitro* behaviour of the I56T variant that is responsible for a form of familial amyloidosis

Christine L.Hagan[1], Russell J.K.Johnson[1], Anne Dhulesia[1], Mireille Dumoulin[2], Janice Dumont[2], Erwin De Genst[1], John Christodoulou[1,3], Carol V.Robinson[1,4], Christopher M.Dobson[1,5] and Janet R.Kumita[1,5]

[1]Department of Chemistry, University of Cambridge, Lensfield Road, Cambridge CB2 1EW, UK, [2]Laboratory of Enzymology and Protein Folding, Centre of Protein Engineering, Institute of Chemistry B6c, University of Liège, B-4000 Liège, Belgium, [3]Present address: Research Department of Structural and Molecular Biology, University College London, Darwin Building, Gower Street, London WC1E 6BT, UK and [4]Present address: Physical and Theoretical Chemistry Laboratory, University of Oxford, South Parks Road, Oxford OX1 3QZ, UK

[5]To whom correspondence should be addressed.
E-mail: jrk38@cam.ac.uk (J.R.K.) or cmd44@cam.ac.uk (C.M.D.)

Received March 8, 2010; revised March 8, 2010; accepted March 14, 2010

Edited by Fabrizio Chiti

We report here the detailed characterisation of a non-naturally occurring variant of human lysozyme, I59T, which possesses a destabilising point mutation at the interface of the α- and β-domains. Although more stable in its native structure than the naturally occurring variants that give rise to a familial form of systemic amyloidosis, I59T possesses many attributes that are similar to these disease-associated species. In particular, under physiologically relevant conditions, I59T populates transiently an intermediate in which a region of the structure unfolds cooperatively; this loss of global cooperativity has been suggested to be a critical feature underlying the amyloidogenic nature of the disease-associated lysozyme variants. In the present study, we have utilised this variant to provide direct evidence for the generic nature of the conformational transition that precedes the ready formation of the fibrils responsible for lysozyme-associated amyloid disease. This non-natural variant can be expressed at higher levels than the natural amyloidogenic variants, enabling, for example, singly isotopically labelled protein to be generated much more easily for detailed structural studies by multidimensional NMR spectroscopy. Moreover, we demonstrate that the I59T variant can readily form fibrils *in vitro*, similar in nature to those of the amyloidogenic I56T variant, under significantly milder conditions than are needed for the wild-type protein.

Keywords: fibril formation/human lysozyme/protein misfolding/systemic amyloidosis

Introduction

The deposition, in a range of tissues and organs, of specific proteins as aggregated species sharing a distinctive fibrillar ultrastructure is a hallmark of an important family of protein misfolding disorders, collectively known as amyloid diseases (Chiti and Dobson, 2006). A variety of such disorders has been identified, including organ-specific conditions such as Alzheimer's disease and type II diabetes, as well as the non-neuropathic systemic amyloidoses associated with the proteins transthyretin and lysozyme (Dobson, 1999). In the case of the latter disorder, it was only in the early 1990s that two single-point mutations (I56T and D67H) in human lysozyme were found to be associated with this familial disease (Pepys *et al.*, 1993; Booth *et al.*, 1997). More recently, other single-point mutations (F57I and W64R) and two double mutations (F57I/T70N and T70N/W112R) have also been linked to this form of amyloidosis (Granel *et al.*, 2002; Valleix *et al.*, 2002; Yazaki *et al.*, 2003; Röcken *et al.*, 2005). Interestingly, two naturally occurring mutations, T70N and W112R, have been identified but do not appear to give rise to any manifestation of disease (Booth *et al.*, 2000; Yazaki *et al.*, 2003).

Human lysozyme is a glycosidase which functions as an antibacterial agent (Fleming, 1922). It contains 130 amino acid residues, and in its native state, the protein possesses four disulphide bonds and consists of two structural domains, a predominantly helical region (the α-domain) and a region containing significant β-sheet structure (the β-domain) (Fig. 1A) (Artymiuk and Blake, 1981). Since their identification, the I56T and D67H variants have been extensively studied *in vitro*, revealing that amyloid formation arises from a reduction, relative to wild-type (WT) lysozyme, both in native state stability and in the global cooperativity of the protein structure. These two mutations cause a similar decrease in native stability (at pH 5.0, the midpoints of thermal denaturation are $10 \pm 1^{\circ}C$ lower than for the WT protein), and both the variants populate an effectively identical, partially unfolded intermediate under physiologically relevant conditions (Canet *et al.*, 1999; Takano *et al.*, 2001a; Canet *et al.*, 2002; Dumoulin *et al.*, 2005; Kumita *et al.*, 2006). In this transient species, the β-domain and the adjacent C-helix are simultaneously unfolded, whereas the regions of the sequence that form helices A, B and D in the remainder of the α-domain maintain significantly native-like structure.

Biophysical analysis of the non-amyloidogenic T70N variant reveals that it is destabilised relative to the WT protein, but only by $4 \pm 1^{\circ}C$, and under physiologically relevant conditions, T70N does not detectably populate the partially unfolded transient intermediate (Esposito *et al.*, 2003; Johnson *et al.*, 2005). Interestingly, at elevated temperatures, the transient intermediate can be significantly populated for this variant as indeed it can, under even more extreme conditions, for the WT protein. These observations indicate that the species involved in this unfolding process, for all these proteins, are closely related to the intermediate previously observed in the folding of WT lysozyme (Hooke *et al.*,

© The Author 2010. Published by Oxford University Press. All rights reserved.
For Permissions, please e-mail: journals.permissions@oxfordjournals.org

Downloaded from http://peds.oxfordjournals.org at Bibliotheque Fac de Medecine on April 11, 2010

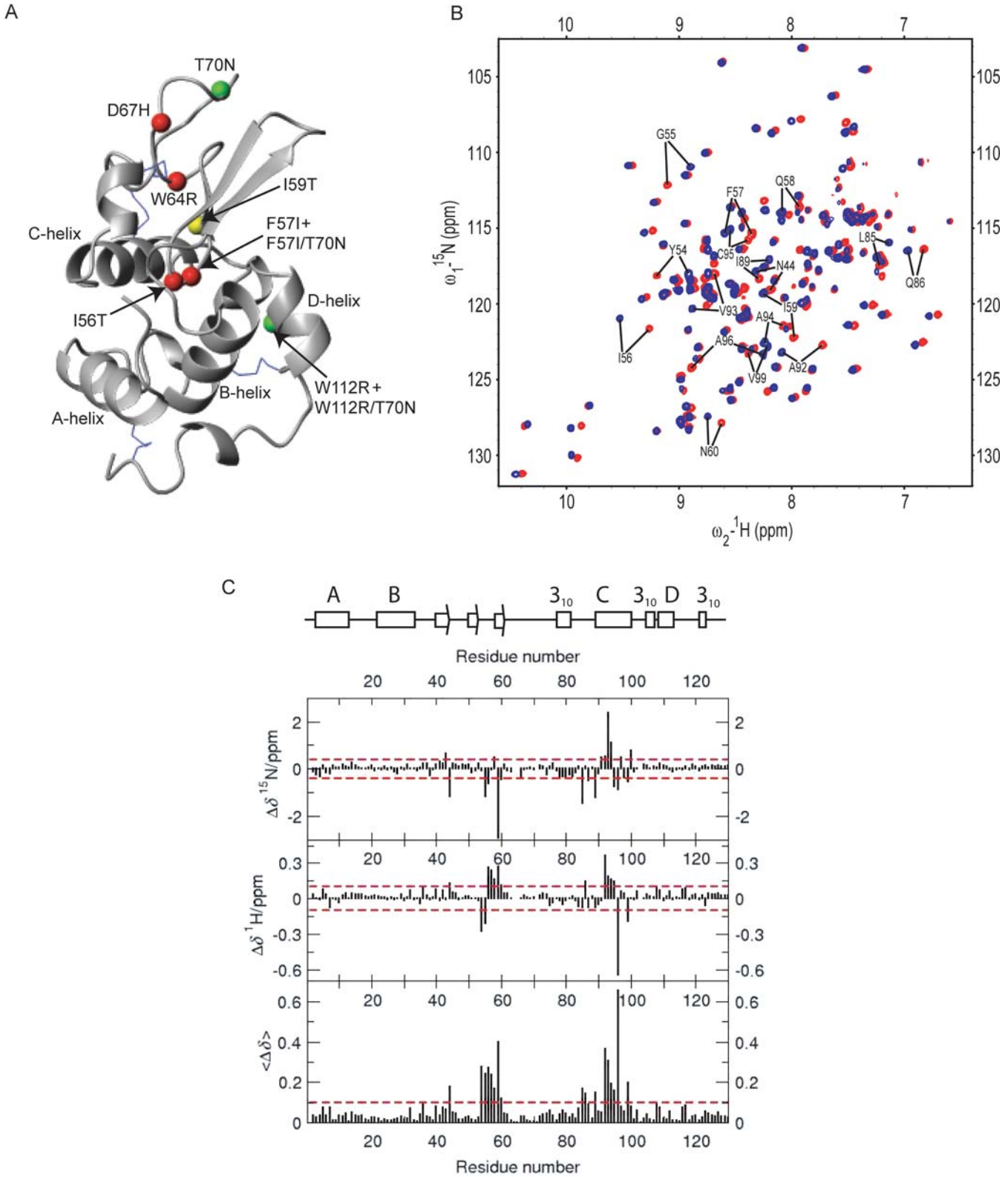

Fig. 1. Location of mutations in human lysozyme and structural comparison of I59T lysozyme with the WT protein. (**A**) The location of the single-point mutations are shown on the structure of human WT lysozyme, defined by X-ray diffraction (PDB entry 1REX). Known native amyloidogenic variants are shown in red, the natural non-amyloidogenic single-point mutations, T70N and W112R, are shown in green and the non-natural I59T mutation, focused on in this study, is shown in yellow. Disulphide bridges are shown as blue lines. The structure was produced using MolMol (Koradi *et al.*, 1996). (**B**) Overlay of the ^{15}N–^{1}H HSQC spectra of the I59T (blue) and the WT protein (red) at pH 5.0, 37°C in 90% 50 mM phosphate buffer and 10% ^2H_2O. The residues showing a significant weighted difference in chemical shifts are labelled. (**C**) Perturbations in chemical shifts measured by NMR for the I59T variant compared with the WT protein; (top) the differences in ^{15}N chemical shift, $\Delta\delta^{15}$N, (middle) differences in ^{1}H chemical shift, $\Delta\delta^1$H, and (bottom) weighted difference $< \Delta\delta >= \sqrt{(\Delta\delta(^{15}\mathrm{N}))^2 + (\Delta\delta(^1\mathrm{H}) \cdot (\gamma(^1\mathrm{H})/\gamma(^{15}\mathrm{N})))^2}$, where γ represents the gyromagnetic ratio of a given nuclei. Chemical shift changes of >0.1 ppm for ^{1}H, 0.4 ppm for ^{15}N and 0.1 ppm for $<\Delta\delta>$ are considered significant, and these boundaries are marked by dotted red lines.

Downloaded from http://peds.oxfordjournals.org at Bibliotheque Fac de Medecine on April 11, 2010

1994; Johnson *et al*., 2005). In order to understand in greater detail the reasons that certain natural lysozyme variants result in amyloid disease, it is important to probe the properties of non-natural variants.

In the previous work, the I59T variant was identified as having a native state stability approximately mid-way between the amyloidogenic variants and the WT protein (Funahashi *et al*., 1999; Takano *et al*., 2001b; Kumita *et al*., 2006). As the I59T mutation is located at the interface of the α- and β-domains, where the naturally occurring amyloidogenic variants I56T and F57I are located, we decided to explore the biophysical characteristics of this non-natural lysozyme variant to gain further insight into the mechanism of *in vitro* lysozyme fibril formation. This study confirms that the native state stability of the I59T variant is lower than that of the WT protein at pH 5.0, interestingly, we have found that this variant populates significantly a transient intermediate species under physiologically relevant conditions similar to that formed by the disease-associated variants, and can also form fibrils *in vitro* under conditions similar to those reported for the amyloidogenic variants, I56T and D67H (Dumoulin *et al*., 2005).

Materials and methods

All chemicals and reagents were purchased from Sigma-Aldrich UK unless otherwise stated.

Protein expression and purification

The I56T, I59T and WT human lysozymes were expressed and purified as previously described (Spencer *et al*., 1999; Johnson *et al*., 2005; Kumita *et al*., 2006) and a large scale batch of I59T lysozyme was expressed in a 15 l fermentor at the Protein Production and Characterization core facility of the Centre for Protein Engineering (University of Liège, http://www.cip.ulg.ac.be/facilities.htm). ^{15}N-labelled I59T lysozyme was expressed in *Pichia pastoris*. Pre-cultures (6 ml) were started in buffered minimal glycerol (BMG) media [100 mM potassium phosphate, pH 6.0, 1.34% yeast nitrogen base (YNB) with 10 g ammonium sulphate, 4×10^{-5}% biotin and 1% glycerol]. These cultures were incubated for 48 h (30°C, 230 rpm) and a 1:100 dilution was made into 500 ml BMG and incubated for 48 h (30°C, 230 rpm). The BMG cultures (250 ml) were centrifuged (5000*g*, 4°C, 10 min) and the supernatant was discarded. The yeast pellets were resuspended in 500 ml buffered minimal methanol media (100 mM potassium phosphate, pH 6.0, 1.34% YNB with 5 g of ^{15}N-labelled ammonium sulphate, 4×10^{-5}% biotin and 0.5% methanol) to induce protein expression and induction was performed for 72 h (30°C, 230 rpm) with 0.5% methanol being replenished every 12–24 h. After induction, the cultures were centrifuged (9000*g*, 4°C, 10 min) and the pellets were discarded. The supernatant was then centrifuged a second time (9000*g*, 4°C, 10 min) and filtered. Purification of lysozyme from the supernatant was performed on an HS20 cation-exchange POROS column (Applied Biosystems, Warrington, UK) on a Biocad 700E system (Applied Biosystems). Lysozyme was eluted at ~55 mS by a linear NaCl gradient. The protein peaks were analysed by SDS–PAGE and the relevant fractions were dialysed against water for 48 h and then lyophilised. The purity of proteins was confirmed by SDS–PAGE and molecular masses were determined by electrospray ionisation mass spectrometry (ESI-MS). For all proteins, stock solutions of lyophilised material were made in Milli-Q water. Stock solutions were passed through 0.22 μm pore size filters and concentrations were determined by UV spectroscopy using an extinction coefficient of 36 940 M^{-1} cm^{-1} at 280 nm for all variants in this study; dilutions into appropriate buffers were made for each assay.

NMR spectroscopy

^{15}N-labelled I59T protein was prepared in 90% 50 mM phosphate buffer, 10% $^{2}H_2O$ and adjusted to pH 5.0. Spectra were recorded at a protein concentration of 630 μM in a Shigemi tube at 37°C. ^{15}N–^{1}H resonance assignment for the I59T variant was achieved by comparison with the known assignments of the closely similar spectrum for the WT protein (Ohkubo *et al*., 1991) and T70N variant (Johnson *et al*., 2005) and supplemented by analysis of standard 3D-NMR experiments (^{15}N–^{1}H, HSQC-NOESY and TOCSY) recorded on a Bruker Avance spectrometer at 700 MHz equipped with a TXI cryoprobe. Additionally, HSQC spectra were recorded on a Bruker Avance spectrometer at 500 MHz equipped with a TCI cryoprobe. The spectra were processed with NMRPipe (Delaglio *et al*., 1995) and viewed with Sparky (http://www.cgl.ucsf.edu/home/sparky/).

Real-time hydrogen/deuterium exchange experiments

Amide hydrogen exchange was monitored for the I59T variant by 2D-NMR. ^{15}N-labelled I59T sample was dissolved in 550 μl of 20 mM acetic acid-d_4 in $^{2}H_2O$, pD 5, to a final concentration of 350 μM and immediately placed in the Bruker Avance 700 MHz NMR spectrometer that was pre-tuned and shimmed with an equivalent sample. A series of HSQC spectra were recorded over time. Hydrogen exchange rates were measured from the reduction of peak volumes over time. Protection factors were calculated from the ratio of experimental rates to the predicted rates for a random coil model based on the primary structure (Bai *et al*., 1993). Ratios of amide protection factors for WT lysozyme were compared with those for the I59T variant.

Thermal denaturation followed by circular dichroism and fluorescence spectroscopy

Thermal denaturation was monitored by circular dichroism (CD) spectroscopy at 222 nm (far-UV) and 270 nm (near-UV) in a Jasco J-810 spectropolarimeter (JASCO Ltd, Great Dunmow, UK). Samples were analysed using 0.1 and 1.0 cm path-length cells, respectively, with a protein concentration of 13.6 μM [10 mM sodium citrate (pH 5.0)]. Far-UV scans were recorded from 200 to 250 nm, and near-UV scans were recorded from 250 to 350 nm; all scans were recorded at 20°C and the spectra reported are the average of five scans each, with appropriate background spectra subtracted. A scan speed of 50 nm min^{-1}, with a 1 nm bandwidth and a 4 s response time, was used. For thermal denaturation, the temperature was increased from 20 to 95°C at a rate of 0.5°C min^{-1} and all experiments were performed in triplicate.

Ellipticity values were normalised to the fraction of unfolded protein (F_u) using $F_u = (\theta - \theta_N)/(\theta_U - \theta_N)$, where θ is the observed ellipticity, θ_N the native ellipticity and θ_U the unfolded ellipticity. θ_N and θ_U were extrapolated from

Downloaded from http://peds.oxfordjournals.org at Bibliotheque Fac de Medecine on April 11, 2010

pre- and post-transition baselines at the relevant temperature. Experimental data were fitted to a sigmoidal expression (Mombelli *et al.*, 1997) using SigmaPlot 9.0 (Systat Software UK Ltd, London, UK). T_m is defined as the temperature where the fraction of unfolded protein is 0.5. Thermal denaturation monitored by 8-anilino-1-napthalenesulfonic acid (ANS) fluorescence emission was recorded on a Cary Eclipse spectrofluorimeter (Varian Ltd, Oxford, UK) using excitation and emission wavelengths of 350 and 475 nm, respectively, and slit-widths of 5 nm. The temperature was increased from 20 to 95°C at a rate of 0.5°C min^{-1} and the analysis performed on 2.0 μM protein in 0.1 M sodium citrate (pH 5.0), containing 360 μM ANS. Transition curves of a control sample of ANS alone (360 μM) were collected and subtracted from all samples to take into account the effects of temperature on ANS fluorescence. The fluorescence data were normalised with respect to the emission spectrum of ANS in the presence of the I56T variant. Experimental data were fitted to a Gaussian expression using SigmaPlot 9.0 (Systat Software UK Ltd). $T_{m\ ANS}$ is defined as the temperature where the intensity of the ANS fluorescence emission is at its maximum value.

Chemical denaturation monitored by intrinsic fluorescence and far-UV CD

Preparation of the samples. The WT, I56T and I59T proteins were incubated overnight at 25°C in sodium phosphate buffer (50 mM, pH 6.5) in the presence of increasing concentrations of guanidinium hydrochloride (GdnHCl). The protein concentration was 1.6, 1.9 and 11 μM for WT, I56T and I59T, respectively. The reversibility of unfolding transitions was checked by diluting the samples from post-transition (6 M) GdnHCl to pre-transition GdnHCl concentrations. Unfolding and refolding curves were determined by monitoring the intrinsic fluorescence emission (for the three proteins) and far-UV CD (only for the I59T variant) at 25°C. The final concentration of GdnHCl was determined by refractometry using $[GdnHCl] = 57.147(\Delta n) + 38.68(\Delta n)^2 - 91.60(\Delta n)^3$, where Δn is the difference between the refractive indices of the GdnHCl solution and the 50 mM sodium phosphate buffer (Pace, 1986).

Fluorescence measurements. Intrinsic fluorescence emission spectra were recorded on a Cary Eclipse spectrofluorimeter (Varian Ltd) in a quartz ultra-micro-cell (Hellma UK Ltd, Southend-On-Sea, UK) with a 1 cm path length. Both excitation and emission slit widths were 5 mm, the scan speed was 600 nm min^{-1} and the photomultiplication was 800 V. The excitation wavelength was 295 nm and emission spectra were recorded from 300 to 440 nm; for each sample, five spectra were accumulated and averaged. Fluorescence spectrum of each sample was corrected for the background fluorescence of the solution (buffer and denaturant).

Five fluorescence parameters have been considered in this work: the fluorescence intensity at 340 and 360 nm, the ratio of fluorescence intensities at 340 and 360 nm, the wavelength corresponding to the maximum in fluorescence intensity (λ_{max}) and the centre of the spectral mass of the fluorescence spectrum (csm) following a procedure previously published (Dumoulin *et al.*, 2002). The analysis based on these five parameters resulted in similar values of thermodynamic parameters, within the error limit, which were averaged to yield the data in Table I.

CD measurements. CD measurements were performed with a Jasco J-810 spectropolarimeter, using a 0.1 cm path-length cell. GdnHCl unfolding curves were recorded at 222 nm. At all denaturant concentrations, at least 30 data points were acquired and averaged with a reading frequency of 0.1 s^{-1}, a 1 s integration time and a 1 nm bandwidth. The resulting values were corrected for the contribution of the solvent.

Data analysis. The thermodynamic parameters for chemical unfolding were computed on the assumption of a two-state model for the unfolding reaction (N⇆U). On this basis, the transition curves were analysed according to the following equation (Pace, 1990):

$$y_{obs} = \frac{(y_N + p[D]) + (y_U + q[D])\exp[a]}{1 + \exp[a]}$$

where

$$a = -\frac{(\Delta G^\circ(H_2O)_{NU} + m_{NU}[D])}{RT},$$

y_{obs} is the measured variable parameter at a given denaturant concentration, and y_N and y_U represent the values of this parameter for the native and denatured states, respectively. $\Delta G^\circ(H_2O)_{NU}$ is the difference in free energy between the folded and unfolded conformations, in the absense of denaturant; m_{NU} is a measure of the dependence of the free energy on the denaturant concentration and $[D]$ the denaturant concentration. p and q are the slopes of the pre- and post-transition baselines, respectively, R the gas constant and T the absolute temperature. The midpoint of the denaturation curve is given by $C_m = \Delta G^\circ(H_2O)/m$. The fraction of unfolded protein (f_U) was calculated according to the following equation:

$$f_U = \frac{y_N - y_{obs}}{y_N - y_U}$$

Table I. Biophysical characteristics of I59T compared with I56T and WT lysozymes

Lysozyme variant	T_m (far-UV CD)	T_m (near-UV CD)	$T_{m\ ANS}$	$\Delta G^\circ(H_2O)_{NU}$ (kJ mol^{-1})	*m*-value (kJ mol^{-1} M^{-1})	C_m (M)
I56T	67.6 ± 0.8[a]	66.0 ± 1.0	65.6 ± 0.9	32.0 ± 3.4	−13.2 ± 1.2	2.4 ± 0.1
I59T	71.0 ± 1.0	69.9 ± 1.0	71.0 ± 0.7	39.3 ± 3.3, 41.1 ± 4.1[b]	−13.1 ± 0.7, −13.6 ± 1.4[b]	3.0 ± 0.1, 3.0 ± 0.1[b]
WT	77.7 ± 0.5	76.7 ± 0.6	79.2 ± 1.5[a]	66.4 ± 3.0	−17.2 ± 0.5	3.9 ± 0.1

[a]Previously reported value under similar conditions (Kumita *et al.*, 2006). All T_m values are measured in °C.
[b]Value obtained from far-UV CD measurements.

Downloaded from http://peds.oxfordjournals.org at Bibliotheque Fac de Medecine on April 11, 2010

Hydrogen exchange monitored by ESI-MS

I56T and I59T variants were deuterated at exchangeable sites by dissolving lyophilised protein (0.2 mg) in ^2H_2O (pH 3.8, 350 μl) and then heating the samples at 70°C for 10 min. After allowing the samples to cool to room temperature, they were flash frozen in liquid N_2 and lyophilised. Prior to performing hydrogen/deuterium (H/D) exchange experiments, the samples were dissolved in ^2H_2O to give protein concentrations of 200 μM. Samples were prepared by manual mixing as described previously (Johnson *et al*., 2005) and spectra were acquired over a mass/charge range of 500–5000 Da on an LCT MS instrument (Waters Ltd, Elstree, UK) equipped with a nanoflow Z-spray source and calibrated with caesium iodide (CsI) (15 μM). The data were analysed using MassLynx 4.0 (Waters Ltd) with molecular masses calculated from the centroid values of at least three charge states. The mass spectra shown represent the convolution of three charged species with minimal smoothing and converted to a mass scale. The per cent population of the intermediate species was calculated using % intermediate species = [(peak intensity of the intermediate species)/(peak intensity of the intermediate species + peak intensity of the native species)] × 100.

Aggregation monitored by right-angle light scattering and thioflavin-T binding

Aggregation studies were performed with the I56T, I59T and WT lysozyme variants [6.8 μM, 0.1 M sodium citrate buffer, pH 5.0, and 62.5 μM thioflavin-T (Thio-T)] incubated with stirring at 60°C in a Cary Eclipse spectrofluorimeter (Varian Ltd). Light scattering was monitored at 500 nm with slit widths of 5 nm and Thio-T fluorescence was measured with an excitation wavelength of 440 nm (slit width 5 nm) and monitored at an emission wavelength of 480 nm (slit width 5 nm). All experiments were performed in triplicate.

Transmission electron microscopy

Samples were applied to Formvar-coated nickel grids, stained with 2% (w/v) uranyl acetate solution and viewed in a Philips CEM100 transmission electron microscope operating at 80 kV as described previously (Dumoulin *et al*., 2003).

Results

As observed previously (Kumita *et al*., 2006), the expression of I59T lysozyme in *P. pastoris* resulted in a significantly higher yield of protein (1.7 ± 0.3 mg l^{-1}) when compared with the amyloidogenic variant, I56T (0.3 ± 0.1 mg l^{-1}). This enabled us to produce singly isotope-labelled ^{15}N-I59T lysozyme in the yeast expression system for multidimensional NMR analysis. The crystal structure of I59T shows that this variant, in its native state, is very similar to that of the WT protein (Funahashi *et al*., 1999). Moreover, analysis of I59T lysozyme by $^1H-^{15}N$ 2D-NMR shows that the WT and I59T spectra overlay for most residues, with some variations in chemical shifts present in the vicinity of residue 59 and in the C-helix region (residues 90–100) (Fig. 1B and C). Far-UV and near-UV CD indicates that the solution structure of this variant also resembles closely that of the WT protein (Supplementary Fig. S1A).

Thermal denaturation, monitored by CD spectroscopy, was determined at pH 5.0; this pH is consistent with recently reported *in vitro* fibril-forming conditions (Dumoulin *et al*., 2005; Kumita *et al*., 2007). As previously demonstrated at pH 2.7 (Funahashi *et al*., 1999), the T_m value at pH 5 for the I59T variant is higher than that of the naturally occurring amyloidogenic variant, I56T, but significantly lower (7 ± 1°C) than that of the WT protein (Supplementary Fig. S1B; Table I). We also monitored the GdnHCl-induced unfolding of the I59T variant using intrinsic fluorescence and far-UV CD (Supplementary Fig. 1C and D). The unfolding transitions obtained by each technique are highly cooperative and occur with full thermodynamic reversibility (data not shown). From these data, we calculated $\Delta G^\circ(H_2O)_{NU}$ values for the I59T variant of 39.3 ± 3.3 and 41.1 ± 4.1 kJ mol^{-1} for fluorescence and far-UV CD, respectively. The superimposition of the CD and fluorescence data after calculation of the fraction of unfolded protein at all denaturant concentrations (Supplementary Fig. 1D) indicates that the secondary and tertiary structures unfold simultaneously, i.e. the transition between native (N) and the unfolded (U) states occurs without populating any intermediate structural states. For comparison, we also measured the GdnHCl-induced unfolding of the I56T and WT proteins by fluorescence measurements (Supplementary Fig. 1C) and the thermodynamic parameters calculated from these data are shown in Table I. Our values of $\Delta G^\circ(H_2O)_{NU}$ for I56T and WT lysozyme at 25°C are comparable with those reported previously by Esposito *et al*. (2003) for I56T and WT lysozyme at 20°C (27.1 ± 0.7 and 57.3 ± 5.7 kJ mol^{-1}, respectively).

By monitoring the ANS binding during thermal denaturation, it has been previously observed that the amyloidogenic variants show strong ANS binding at temperatures close to their T_m values, whereas the WT protein shows very little ANS binding (Dumoulin *et al*., 2005; Kumita *et al*., 2006). Here, we observe an increase in ANS fluorescence emission for the I59T variant due to the appearance of one or more partially unfolded intermediates with solvent-exposed hydrophobic clusters (Fig. 2). This increase in emission signal is, however, only about 60% of that seen for natural amyloidogenic variant, I56T.

For the amyloidogenic variants, I56T and D67H, a partially unfolded transient intermediate is detectable under physiologically relevant conditions by H/D exchange, monitored by mass spectrometry (Canet *et al*., 2002; Dumoulin *et al*., 2005). In these experiments, the proteins are fully deuterated and the exchange monitors the loss of deuterons (as they are replaced by hydrogens) over time. For the amyloidogenic variants, two species have been detected in such experiments; one of which can be attributed to the native state, in which more deuterons are protected, and the other to a species having less deuterons protected and represents the molecules that have, at least once, formed the partially unfolded intermediate species (Miranker *et al*., 1993; Canet *et al*., 1999). There is considerable evidence that the formation of such an intermediate is an important contributor to the process of fibril formation by the amyloidogenic variants of human lysozyme (Dumoulin *et al*., 2005; Chan *et al*., 2008). It has been demonstrated, for example, that stabilisation of the native state of these variants with camelid antibody fragments abolishes the formation of this intermediate, and in addition, strongly inhibits *in vitro* fibril formation

Downloaded from http://peds.oxfordjournals.org at Bibliotheque Fac de Medecine on April 11, 2010

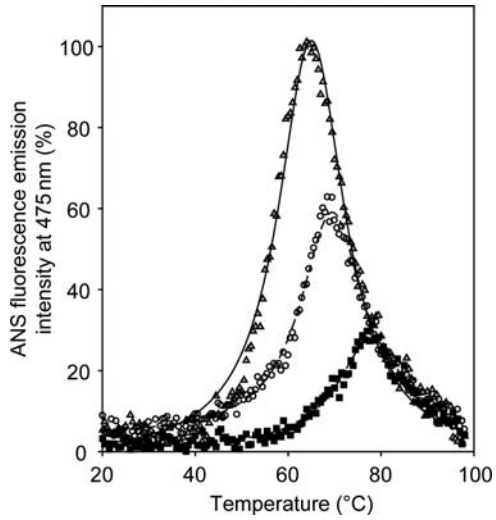

Fig. 2. Identification of partially unfolded intermediates as observed by ANS fluorescence emission. Thermal denaturation as monitored by ANS binding at pH 5.0. All the curves were normalised with respect to the maximum fluorescence value (obtained at the T_m) of the I56T variant. As the amyloidogenic variant, I56T (open triangles), unfolds, we observe a strong ANS fluorescence emission at 475 nm at the temperature that corresponds to the T_m of the protein. The I59T variant (open circles) shows significant ANS signal (albeit not as intense as that of the I56T variant) and the WT protein (filled squares) shows a much lower signal.

(Dumoulin *et al.*, 2003, 2005; Chan *et al.*, 2008). In addition, neither the more stable T70N variant nor the WT protein displays a detectable intermediate under these conditions (Johnson *et al.*, 2005). We report here that the analogous intermediate of I59T is readily detectable at 37°C in the H/D exchange experiment (Fig. 3A). The rate of formation of the intermediate species for I59T is, however, slower than that of the I56T variant with time constants (τ) of 212.8 ± 4.5 and 30.0 ± 2.5 s, respectively (Fig. 3B).

H/D exchange can be monitored in a residue-specific manner using 2D-NMR spectroscopy (Krishna *et al.*, 2004). In these experiments, the rates of exchange (from hydrogen to deuteron) were determined at 37°C and pD 5.0, and from these rates, exchange protection factors were determined based on the rate of exchange in the species being studied relative to the rates of the same amide proton atoms in the unstructured (random coiled) state (Mine *et al.*, 2000). The ratios of the protection factors for amides in I59T relative to those in the WT protein were determined (Fig. 3C), and significant changes in exchange rate as a consequence of the I59T mutation are indicated as being greater than a 10-fold increase. In a similar fashion to the amyloidogenic variants (I56T and D67H), the region that displays the greatest increase in exchange rates is located in the region of residues 39–84, which corresponds to the β-domain of the protein and the region which has been shown to be unfolded in the transiently partially unfolded intermediate (Canet *et al.*, 2002). In the I56T and D67H proteins, residues within the C-helix also show increased exchange rates (Dumoulin *et al.*, 2005), whereas the I59T variant shows values that are increased by <10-fold, indicating that this region is more stable in the latter variant. From the mass spectrometry experiments, the number of protected sites for the intermediate species of I56T and I59T are identical (25 ± 1, as determined at the time point when the population of the native species and

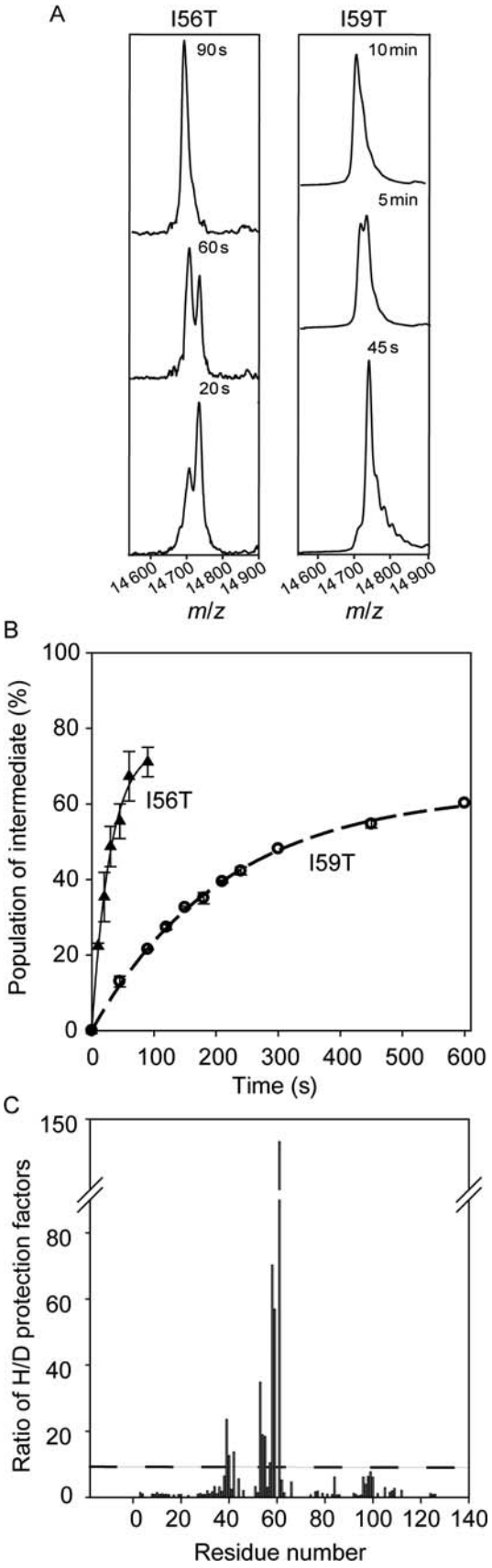

Fig. 3. Appearance of the transient intermediate in lysozyme variants. (**A**) Time points of H/D exchange reactions as monitored by mass spectrometry for I56T (left panel) and I59T (right panel) at 37°C. For the I56T and I59T variants, a higher mass species dominates initially (at 20 and 45 s of exchange, respectively). As time increases, the intensity of the lower mass

Downloaded from http://peds.oxfordjournals.org at Bibliotheque Fac de Medecine on April 11, 2010

intermediate species are similar in intensity), suggesting that in this case, both the C-helix and the β-domain are unfolded; however, the increased stability in the C-helix may explain the slower rate of intermediate formation.

Finally, we wished to define the conditions under which the I59T variant could form fibrils and whether such fibrils are similar in morphology to those formed from one of the amyloidogenic variants (I56T). Previously, lysozyme fibrils have been formed *in vitro* under a number of different destabilising conditions including elevated temperatures and low pH, elevated temperatures and the presence of chemical denaturants and for the amyloidogenic variants, and elevated temperatures only at pH 5.0 (Morozova-Roche *et al.*, 2000; Dumoulin *et al.*, 2003, 2005; Kumita *et al.*, 2007; Frare *et al.*, 2009). Owing to the higher native state stability and slower rate of transient intermediate formation for the I59T variant, we investigated fibril formation with stirring at 60°C, pH 5.0. Light scattering, Thio-T binding and transmission electron microscopy (TEM) confirm that the I59T variant readily forms fibrillar species under these conditions at a slightly slower rate of formation than the I56T variant (Fig. 4). The resulting fibrils are structurally similar to those observed for the I56T variant under the same conditions as determined by TEM analysis (Fig. 4C). WT protein under these conditions did not aggregate over the time course of 500 min. The ability of the I59T variant to form fibrils over a time course of hours rather than days is extremely valuable for probing important issues such as the ability of compounds to inhibit this process (Kumita *et al.*, 2007; Yerbury *et al.*, 2009). This allows us to study how biological factors can influence fibril formation, thereby shedding light on how living systems have evolved to deal with protein misfolding.

Discussion

Two key attributes have been found to be important for *in vitro* fibril formation by the amyloidogenic variants, I56T and D67H, namely a decrease in native state stability and a loss in global cooperativity, both leading to the population of a transient intermediate species (Dumoulin *et al.*, 2003, 2005). This partially unfolded intermediate is not, in itself, unique to the amyloidogenic variants; in fact, under destabilising conditions (such as high temperatures or low pH), this intermediate is detectable even for the WT protein (Johnson *et al.*, 2005). The I59T variant, examined in the present study, like the disease-associated variants, possesses this attribute under physiological conditions, albeit with a slower rate of formation than the I56T variant. Moreover, the I59T variant can reproducibly form fibrils on a relatively fast time scale *in vitro* ($t_{1/2} = 170 \pm 40$ min at 60°C, pH 5.0) in the absence of chemical denaturants, providing a valuable assay for investigating factors which can alter fibril formation. Indeed, it has allowed us to study the inhibitory effects of the extracellular chaperones, clusterin, haptoglobin and α_2-macroglobulin under conditions that do not perturb the activity of these chaperones (Kumita *et al.*, 2007; Yerbury *et al.*, 2009).

It is interesting that the I59T variant is more stable than the I56T protein as the locations of these mutations are in a similar region of the protein, completely buried in the interior of the molecule. Analysis of the X-ray structures shows, however, that the side-chain packing around Ile56 is

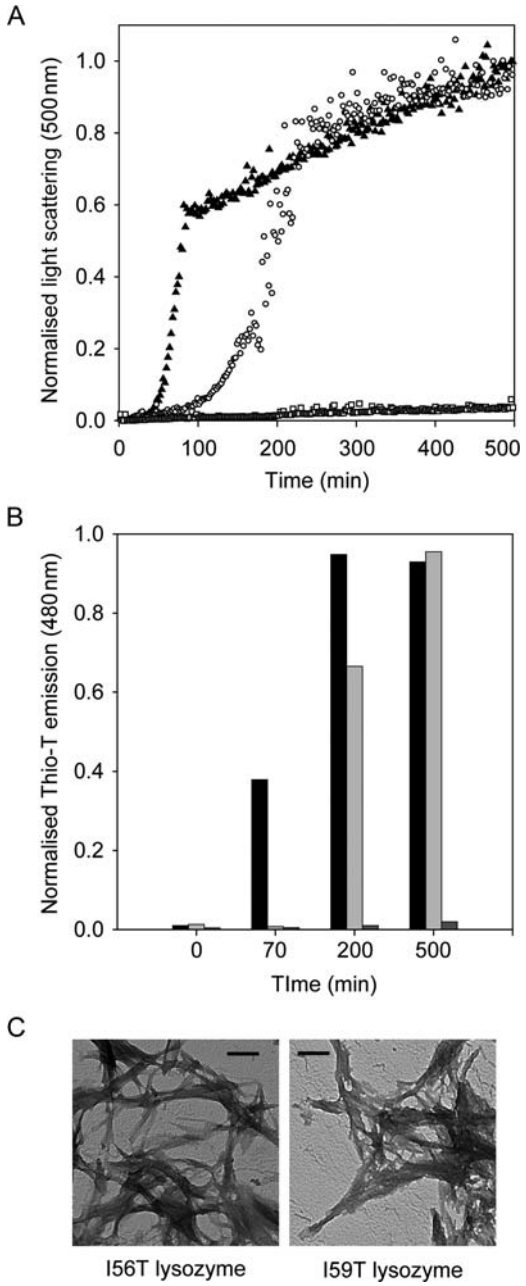

Fig. 4. *In vitro* fibril formation of I59T lysozyme. (**A**) Fibril formation monitored by light scattering at 500 nm over time for I56T (filled triangles), I59T (open circles) and WT protein (open squares) at 60°C, pH 5.0. (**B**) Thio-T fluorescence measured at various time points throughout the light-scattering assay for I56T (black bars), I59T (light grey bars) and WT (medium grey bars). (**C**) TEM analysis of samples taken at the end of the growth phase observed in the light-scattering assay for I56T and I59T variants. The scale bar represents 200 nm.

species increases; albeit at different rates for each variant. (**B**) The populations of the intermediate states are plotted versus time to determine the rate of formation of the transient intermediate. The time constant of unfolding ($\tau = 1/k$) for I56T (solid triangles) and I59T (open circles) are 30.0 ± 2.5 and 212.8 ± 4.5 s, respectively. (**C**) Ratios of amide protection factors for the WT lysozyme compared with those of the I59T variant. The broken line represents the value for which amide groups of the WT protein have protection factors 10 times those of the I59T variant. A ratio of 1.0 represents an equal degree of protection in both proteins.

Downloaded from http://peds.oxfordjournals.org at Bibliotheque Fac de Medecine on April 11, 2010

tighter than that of Ile59; this suggests that the insertion of different side chains may not be as easily accommodated (Funahashi *et al*., 1999). Indeed, a cavity in the structure is formed by the I56T mutation, whereas in I59T, a rearrangement is observed in which the hydroxyl group of the introduced threonine forms a hydrogen bond with a newly introduce water molecule (Funahashi *et al*., 1999). Previous studies have demonstrated that a water molecule in a cavity created in the interior of lysozyme contributes favourably to stability (Takano *et al*., 1997). Regardless of the origin of the extra stability afforded to the I59T variant, its intermediate nature in terms of biophysical characteristics provides us with a strategy through which we can begin to understand, *in vitro*, the fundamental effects of mutations in the interface region and to investigate the degree to which the loss of native state stability and the ability to populate a transient intermediate species is necessary to promote the amyloidogenic character of certain lysozyme variants.

Supplementary data

Supplementary data are available at *PEDS* online.

Acknowledgements

We would like to thank Alain Brans and Fabrice Boullienne at the University of Liège for their assistance with protein expression.

Funding

This research was supported in part by a grant from the Biotechnology and Biological Sciences Research Council (BB/EO19927/1 to C.M.D., C.V.R. and J.R.K.), Programme grants from the Wellcome Trust, the European Commission (project LSHM-CT-2006-037525) and the Leverhulme Trust (to C.M.D.), the Belgian Government under the framework of the Interuniversity Attraction Poles (I.A.P. P6/19) (to C.M.D. and M.D.), the Winston Churchill Foundation (to C.L.H.), a BBSRC studentship (to R.J.K.J.), Boerhinger Ingelheim Funds (to A.D.) and an EMBO long-term postdoctoral fellowship and a Marie Curie Intra European fellowship (to E.D.G). J.D. is supported by the Belgian *Fonds de la Recherche pour les Industries et l'Agriculture* and M.D. is a research associate of the Belgian F.R.S-FNRS.

References

Artymiuk,P.J. and Blake,C.C.F. (1981) *J. Mol. Biol.*, **152**, 737–762.
Bai,Y., Milne,J.S., Mayne,L. and Englander,S.W. (1993) *Proteins*, **17**, 75–86.
Booth,D.R., *et al*. (1997) *Nature*, **385**, 787–793.
Booth,D.R., Pepys,M.B. and Hawkins,P.N. (2000) *Hum. Mutat.*, **16**, 180.
Canet,D., Sunde,M., Last,A.M., Miranker,A., Spencer,A., Robinson,C.V. and Dobson,C.M. (1999) *Biochemistry*, **38**, 6419–6427.
Canet,D., Last,A.M., Tito,P., Sunde,M., Spencer,A., Archer,D.B., Redfield,C., Robinson,C.V. and Dobson,C.M. (2002) *Nat. Struct. Biol.*, **9**, 308–315.
Chan,P.-H., *et al*. (2008) *Biochemistry*, **47**, 11041–11054.
Chiti,F. and Dobson,C.M. (2006) *Annu. Rev. Biochem.*, **75**, 333–366.
Delaglio,F., Grzesiek,S., Vuister,G.W., Zhu,G., Pfeifer,J. and Bax,A. (1995) *J. Biomol. NMR*, **6**, 277–293.
Dobson,C.M. (1999) *Trends Biochem. Sci.*, **24**, 329–332.
Dumoulin,M., Conrath,K., Meirhaeghe,A.V., Meersman,F., Meremans,K., Frenken,L.G.J., Muyldermans,S., Wyns,L. and Matagne,A. (2002) *Protein Sci.*, **11**, 500–515.
Dumoulin,M., *et al*. (2003) *Nature*, **424**, 783–788.
Dumoulin,M., *et al*. (2005) *J. Mol. Biol.*, **346**, 773–788.
Esposito,G., *et al*. (2003) *J. Biol. Chem.*, **278**, 25910–25918.
Fleming,A. (1922) *Proc. R. Soc. Lond. B*, **93**, 306–317.
Frare,E., Mossuto,M.F., Laureto,P.P.d., Tolin,S., Menzer,L., Dumoulin,M., Dobson,C.M. and Fontana,A. (2009) *J. Mol. Biol.*, **387**, 17–27.
Funahashi,J., Takano,K., Yamagata,Y. and Yutani,K. (1999) *Protein Eng.*, **12**, 841–850.
Granel,B., *et al*. (2002) *Gastroenterology*, **123**, 1346–1349.
Hooke,S.D., Radford,S.E. and Dobson,C.M. (1994) *Biochemistry*, **33**, 5867–5876.
Johnson,R.J.K., *et al*. (2005) *J. Mol. Biol.*, **352**, 823–836.
Koradi,R., Billeter,M. and Wuthrich,K. (1996) *J. Mol. Graph.*, **14**, 29–32.
Krishna,M.M.G., Hoang,L., Lin,Y. and Englander,S.W. (2004) *Methods*, **34**, 51–64.
Kumita,J.R., Johnson,R.J.K., Alcocer,M.J.C., Dumoulin,M., Holmqvist,F., McCammon,M.G., Robinson,C.V., Archer,D.B. and Dobson,C.M. (2006) *FEBS J.*, **273**, 711–720.
Kumita,J.R., Poon,S., Caddy,G.L., Hagan,C.L., Dumoulin,M., Yerbury,J.J., Stewart,E.M., Robinson,C.V., Wilson,M.R. and Dobson,C.M. (2007) *J. Mol. Biol.*, **369**, 157–167.
Mine,S., Ueda,T., Hashimoto,Y. and Imoto,T. (2000) *Protein Sci.*, **9**, 1669–1684.
Miranker,A., Robinson,C.V., Radford,S.E., Aplin,R.T. and Dobson,C.M. (1993) *Science*, **262**, 896–900.
Mombelli,E., Afshar,M., Fusi,P., Mariani,M., Tortora,P., Connelly,J.P. and Lange,R. (1997) *Biochemistry*, **36**, 8733–8742.
Morozova-Roche,L.A., Zurdo,J., Spencer,A., Noppe,W., Receveur,V., Archer,D.B., Joniau,M. and Dobson,C.M. (2000) *J. Struct. Biol.*, **130**, 339–351.
Ohkubo,T., Taniyama,Y. and Kikuchi,M. (1991) *J. Biochem. (Tokyo)*, **110**, 1022–1029.
Pace,C.N. (1986) *Methods Enzymol.*, **131**, 266–280.
Pace,C.N. (1990) *Trends Biochem. Sci.*, **8**, 93–98.
Pepys,M.B., *et al*. (1993) *Nature*, **362**, 553–557.
Röcken,C., Becker,K., Fändrich,M., Schroeckh,V., Stix,B., Rath,T., Kähne,T., Dierkes,J., Roessner,A. and Albert,F.W. (2005) *Hum. Mutat.*, **27**, 119–120.
Spencer,A., Morozova-Roche,L.A., Noppe,W., MacKenzie,D.A., Jeenes,D.J., Joniau,M., Dobson,C.M. and Archer,D.B. (1999) *Protein Expr. Purif.*, **16**, 171–180.
Takano,K., Funahashi,J., Yamagata,Y., Fujii,S. and Yutani,K. (1997) *J. Mol. Biol.*, **274**, 132–142.
Takano,K., Funahashi,J. and Yutani,K. (2001a) *Eur. J. Biochem.*, **268**, 155–159.
Takano,K., Yamagata,Y. and Yutani,K. (2001b) *Biochemistry*, **40**, 4853–4858.
Valleix,S., Drunat,S., Philit,J.B., Adoue,D., Piette,J.C., Droz,D., MacGregor,B., Canet,D., Delpech,M. and Grateau,G. (2002) *Kidney Int.*, **61**, 907–912.
Yazaki,M., Farrell,S.A. and Benson,M.D. (2003) *Kidney Int.*, **63**, 1652–1657.
Yerbury,J.J., Kumita,J.R., Meehan,S., Dobson,C.M. and Wilson,M.R. (2009) *J. Biol. Chem.*, **284**, 4246–4254.

Downloaded from http://peds.oxfordjournals.org at Bibliotheque Fac de Medecine on April 11, 2010